Available online at www.sciencedirect.com
SCIENCE DIRECT
Solid State Ionics 177 (2006) 65 – 71
SOLID STATE IONICS
www.elsevier.com/locate/ssi

Study of EVOH based single ion polymer electrolyte: Composition and microstructure effects on the proton conductivity

Yu-jun Zhang [a], Yu-dong Huang [a,*], Lei Wang [b]

[a] *Department of Applied Chemistry, Harbin Institute of Technology, P.O. Box 410, Xidazhi Street 92, Nangang District, Harbin 150001, China*
[b] *School of Materials Science and Engineering, Harbin University of Science and Technology, P.O. Box. 3491, Linyuan Road 4, Dongli District, Harbin 150040, China*

Received 1 July 2005; received in revised form 1 October 2005; accepted 8 October 2005

Abstract

A comb-like EVOH based single ion polymer electrolyte (EVOH-*g*-SPEG) was synthesized by sulfonification of EVOH grafts 2-(2-chloroethoxy) ethanol ($C_4H_9O_2Cl$)/2-[2-(2-chloroethxy) ethoxy] ethanol ($C_6H_{13}O_3Cl$) with 1, 3-propane sultone. The main chain of the comb-like polymer is hydrophobic polyethylene segments; the side chain is hydrophilic poly (ethylene glycol) (PEG) segment, which can solubilize large amounts of inorganic salts. The sulfonic acid group was introduced onto the end of the PEG side chain. The acid form of SPE was successfully obtained by being dialyzed from the products with acid solution. The saturation water sorption of EVOH-*g*-SPEG membrane increased with the side chain length and the immersion time. The XRD results indicate that the water in SPE membrane region can destroy the membrane crystalline structure and the water absorption membranes are nearly amorphous. AFM phase images of the hydration membranes clearly show the hydrophilic domains, with sizes increasing from 10 to 35 nm as a function of the side chain length. A phase inversion could be observed when $n \geq 5$, which was consistent with a rapid increase in water absorption. And the ion conductivity is also measured by AC impedance. The conductivity is greatly influenced by ion exchange capacity and water sorption. The comb-like EVOH-*g*-SPEG polymer electrolyte grafts with 2 PEG side chain provides the highest ionic conductivity (1.65×10^{-3} S cm^{-1}). The comb-like polymer could be a candidate as new polymeric electrolyte material for fuel cells and other electrochemical devices.

Keywords: EVOH-*g*-SPEG; PEG; Polymer electrolyte; Impedance spectroscopy

1. Introduction

Since the discovery of ionic conductivity in some polyether-based polymer hosts with alkali metal salts by Fenton et al. [1] and Armand [2], solid polymer electrolytes (SPE) have been the subject of numerous studies relating to lithium ion polymer batteries [3], capacitors [4,5], and electrochemical devices [6]. Polymer electrolytes not only have relatively high ionic conductivity in the solid state but also have characteristic properties such as process ability, flexibility, light weight, elasticity and transparency. However, in ordinary polymer electrolytes, both the cation and anion are mobile. If such bi-ionic conductors are applied to the recharge lithium batteries, the migration of anions causes concentration gradient of the electrolyte salts and polarization of the batteries [7]. To improve the charge–discharge performance of lithium polymer electrolyte battery, single ion conducting polymer electrolyte was used instead of a bi-ionic conductors. Nafion, a commercially available single ion solid polymer electrolyte, has been widely used in fuel cell applications since the perfluorinated ionomer membranes have a high chemical and electrochemical resistance at harsh operating conditions, as well as high proton conductivity (~0.1 S/cm) [8]. However, the high costs of Nafion bring about the limit for their application. Thus, the development of cheaper single ion solid polymer electrolytes becomes more important.

Most previous studies have focused on the modified form of poly (ethylene glycol) (PEG) and poly (propylene glycol) (PPG) because of their ability to solubilize large amounts of inorganic salts. Polyanionic salts were blended or alloyed with high molecular weight PEO to achieve practical single ion

* Corresponding author. Tel.: +86 451 86392586.
E-mail address: zhangyujun2003@163.com (Y. Huang).

0167-2738/$ - see front matter © 2005 Elsevier B.V. All rights reserved.
doi:10.1016/j.ssi.2005.10.008

conductors [9,10]. Anions have also been attached to the linear PEO chain ends [11], tethered to side chains of the comb-branched polymers [12], fixed to the polymer mainchains [13,14] or between polymer chains as a crosslinker [15], were copolymerized with non-ionic units containing oligoethylene oxide units [16], or fixed to fumed silica nanoparticles to form composite single ion conductors [17]. An alternative method to form single ion conductors is to form nanocomposites between natural clays and polymers thereby taking advantage of the ion exchange capacity of the clay and the solvating power of the polymer to provide lithium ion mobility [18–21]. The best ambient conductivities reported for these single ion conductors are in the range of 10^{-6} to 10^{-5} S cm^{-1}. Derand et al. [22] reported a comb-like polymer prepared by ethoxylation of EVOH with side chain end-capped with sulfonic acid groups; they indicated its potential application in recharge lithium batteries while our interest in the work is on the potential application of such a polymer electrolyte with controlled side chain length in fuel cell membranes. For this purpose, a comb-like EVOH-*g*-SPEG single ion polymer electrolyte was synthesized by sulfonification of EVOH grafts 2-(2-chloroethoxy) ethanol ($C_4H_9O_2Cl$)/2-[2-(2-chloroethxy) ethoxy] ethanol ($C_6H_{13}O_3Cl$) with 1, 3-propane sultone in this study. It is anticipated that the comb-like single ion polymer electrolyte with controllable side chain length should provide higher proton conductivity. The relationship of ionic conductivities and the length of the side chain will be discussed by AC impedance, and the morphology of ionic cluster in electrolyte membrane will be also studied by AFM in this paper.

2. Experimental

2.1. Materials

EVOH used in this study was poly (ethylene-co-vinyl alcohol) from Japan STS (68 mol% vinyl alcohol,). 2-(2-chloroethoxy) ethanol ($C_4H_9O_2Cl$)/2-[2-(2-chloroethxy) ethoxy] ethanol ($C_6H_{13}O_3Cl$) was purchased from Aldrich Co., Germany. 1, 3-propane sultone was purchased from Fengfan Chemical Co. Potassium *tert*-butoxide purchased from Acros Organics (95–99%). Dimethyl acetamide (DMAc) was purchased from Tianjin Kaitong Chemical Reagent Factory.

2.2. Synthesis of EVOH-g-SPEG

The comb-like polymer electrolyte was synthesized by a two-step process. EVOH was dried in vacuum for 12 h at 60 °C and then dissolved in DMAc. The catalyst NaOH, corresponding to 50 mol% of the hydroxyl reactive groups of the polymer, was dissolved in DMAc and added to the polymer solution under stirred. Then the 2-(2-chloroethoxy) ethanol ($C_4H_9O_2Cl$) or 2-[2-(2-chloroethxy) ethoxy] ethanol ($C_6H_{13}O_3Cl$) was slowly dropped into the transparent mixture solution through a syringe. The reaction was allowed to continue for 2 h with the solution color changing from transparency to thin yellow. And then quantitative potassium *tert*-butoxide dissolved in DMAc for 1 h under 60 °C was added to the reaction solution. The reaction mixtures were heated to 80 °C before addition of 1, 3-propane sultone and then allowed to proceed for 12 h at 80 °C (the reaction scheme is shown in Scheme 1). To get a comb-like EVOH-*g*-SPEG polymer electrolyte with more than 3 PEG side chains, another Williamson reaction will be carried basing on the intermediate compound of EVOH-*g*-SPEG with 2/3 PEG units. It is reported [23,24] that the side chain with 6/7 PEG repeat units tend to crystallize more easily which will decrease the proton conductivity ability of the polymer electrolyte. So the numbers of PEG units on the resulting polymer in this experiment will be controlled fewer than 6. The products were dialyzed using dialyzer bag (cut-off value is 14,000) in deionized water to removed the small molecular weight substances, and than dialyzed in acid solution to obtain the acid form of the electrolyte.

2.3. Preparation of the SPE membrane

EVOH-*g*-SPEG electrolyte membranes were prepared by solution casting using DMAc (10% w/w) on Teflon plates. Solvent removal were done under reduced pressure at gradually increasing temperatures, at 30 °C for 2 h, 50 °C for 2 h, 80 °C for 2 h and 100 °C for 12 h, respectively. The drying procedure was optimized to produce flat and transparent membranes.

2.4. Gel permeation chromatography (GPC)

The molecular weight and molecular weight distribution of the polymer electrolyte were determined by GPC. The samples were dissolved in a DMAc solution at a concentration of 2.0 mg/ml. The solution was filtered through a syringe filter. GPC analyses were carried out using Agilent 1100 using PS columns (styrogel 5 μm diameter). The DMAc solution was used as the fluent at a flow rate of 1 ml/min driven by a pump. The injection volume was 50 μm.

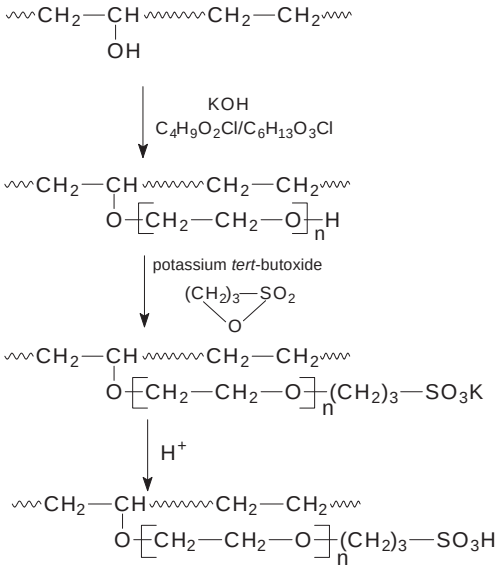

Scheme 1. Synthesis schematic of EVOH-*g*-SPEG ($n=2\sim6$, n represents the number of the grafted PEG segment on the side chain).

Table 1
Structure characteristics of EVOH-*g*-SPEG

Sample	Graft ratio[a] (%)	$\bar{M}_n \times 10^{-4}$	PDI
EVOH	–	8.6	1.3312
EVOH-*g*-SPEG ($n=2$)	42.5	9.9	1.4569
EVOH-*g*-SPEG ($n=3$)	41.7	11.4	1.4608
EVOH-*g*-SPEG ($n=4$)	42.3	13.1	1.5743
EVOH-*g*-SPEG ($n=5$)	42.1	14.5	1.6348
EVOH-*g*-SPEG ($n=6$)	41.8	16.2	1.8783

[a] Graft ratios of the polymer electrolyte were evaluated by GPC.

2.5. Fourier transform infra-red (FTIR) spectroscopy

FTIR spectroscopy was used to confirm the pendant functional groups on the copolymers. Measurements were taken at ambient temperature using a NEXUS 670 equipment at 1 cm^{-1} resolution and 32 scans. For the transmission measurement, polymer samples cast on KBr discs from DMAc solutions were used.

2.6. X-ray diffraction measurement

X-ray diffraction (XRD) measurements were carried out using Philips PW1830 X-ray diffractometer using a Cu Kα-source operated at 40 keV and at a scan rate of 0.1°/s.

2.7. Water uptake of SPE membranes

The EVOH-*g*-SPEG membranes were vacuum-dried at 100 °C for 24 h, weighed and immersed in deionized water at room temperature for 24 h. The wet hydration membranes were wiped dry and quickly weighed again. The water uptakes of membranes are reported in weight percent as follows:

$$\textit{Water uptake} = \frac{W_{\text{wet}} - W_{\text{dry}}}{W_{\text{dry}}} \times 100\%$$

where W_{wet} and W_{dry} are the weights of the wet and dry membranes, respectively.

2.8. IEC values of SPE membranes

The ion exchange capacity (IEC) was obtained from the titration of the released amount of proton (H^+) of the per-

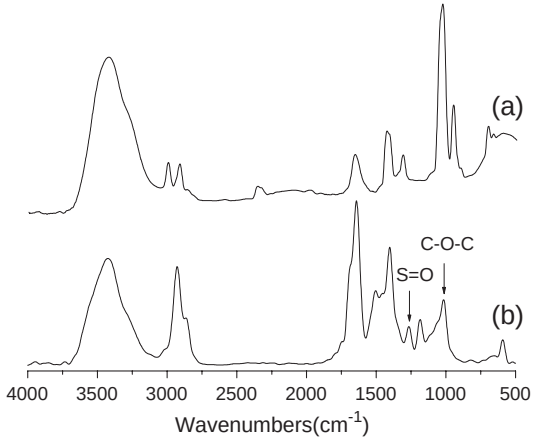

Fig. 1. IR spectra for (a) EVOH and (b) EVOH-*g*-SPEG.

Table 2
Observed wave numbers of EVOH-*g*-SPEG

Wave number (cm^{-1})	Assignment
3426	–OH stretching vibration
2944	Antisymmetric CH_2 stretching vibration
2868	Symmetric CH_2 stretching vibration
1437	–CH in-plane bending vibration of $-CH_2-$
1406	–CH out-of-plane bending vibration of $-CH_2-$
1394	S=O stretching vibration
1313	—CH(OH)— bending vibration
1264	Antisymmetric $-SO_3^-$ stretching vibration
1091	–C–O stretching vibration of the ethereal C–O–C
1028	—CH(OH)— stretching vibration
1013	Symmetric $-SO_3^-$ stretching vibration

weighted polymer in an acid form in 1 M sodium chloride (NaCl) with 0.01 M sodium hydroxide (NaOH) by using a phenolphthalein indicator. The IEC value was recorded as an average value for each sample in units of milliequivalents NaOH per gram of the polymer (mmol/g).

2.9. Atomic force microscopy (AFM)

The AFM equipment used here was a Solver P47 model AFM instrument from NT-MDT Co. (Russia). The membrane morphologies were imaged in tapping mode, using micro-fabricated cantilevers with a force constant of approximately 40 N/m. The ratio of amplitudes used in feedback control was adjusted to 0.6 of the free air amplitude for all the reported images. All samples were dried at 80 °C for 24 h under vacuum conditions. The samples were then imaged immediately in relative humidity of about 35%.

2.10. AC impedance measurements

Impedance measurements of the polymer electrolytes were performed on films made by casting method. The film thickness was maintained in the range of 107–147 ìm and the contact area was controlled at 1.1304 cm^2. Conductivity measurements were performed on membranes fixed between

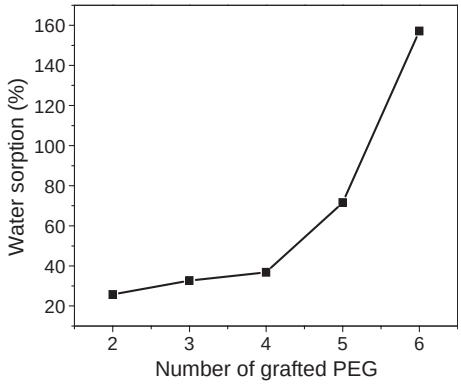

Fig. 2. Water sorption of the polymer membranes with different grafts length of PEG side chains.

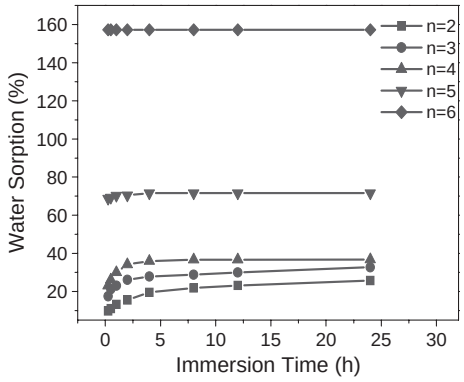

Fig. 3. Water sorption with immersed time under of different grafts length of PEG side chains.

Teflon cell holders attached with stainless steel (SS). This cell geometry was chosen to ensure that the membrane resistance dominated the response of the system. The electrochemical cell was connected at an EG and G PAR model 273 A potentiostat/galvanostat and at a Solartron 1255 frequency response analyzer (FRA) that was interfaced to an IBM PC via a National Instruments IEEE-488 GPIB card. The EG and G PAR-M398 Electrochemical Impedance Software was used for the impedance measurements between 100 kHz and 10 Hz. The amplitude of the AC voltage was 5 mV.

3. Results and discussion

3.1. Molecular weights and graft ratio of EVOH-g-SPEG

The molecular weights and its distribution of EVOH-*g*-SPEG were determined by using GPC and the results were showed in Table 1. The graft ratio of PEG on EVOH-*g*-SPEG is lower than the theoretical value (50%) for the steric restriction between the side chains.

3.2. FTIR study of EVOH-g-SPEG comb-like polymer

The chemical structures of the EVOH-*g*-SPEG were studied by FTIR spectroscopy. Fig. 1 shows the FTIR spectrum of EVOH (curve a) and EVOH-*g*-SPEG (curve b) at room temperature, and some feature wave numbers of EVOH-*g*-SPEG are labeled in Table 2. In all spectra, the peak relevant to the hydrogen-bonded O–H stretching vibration is at about 3400 cm^{-1}, the antisymmetric and symmetric C–H stretching vibration of the CH_2 groups is at 2944 and 2868 cm^{-1}, and the bending bands at 1470~1700 cm^{-1}. The new peak appeared at 1091 cm^{-1} as a broad peak for EVOH-*g*-SPEG is due to the C–O stretching vibration of the ethereal C–O–C. The peak identified in the spectra at 1394 cm^{-1} is due to the asymmetric

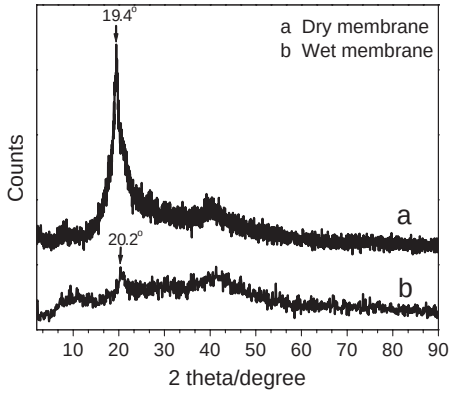

Fig. 4. XRD results of dry and wet polymer membranes of $n=2$ polymer electrolyte.

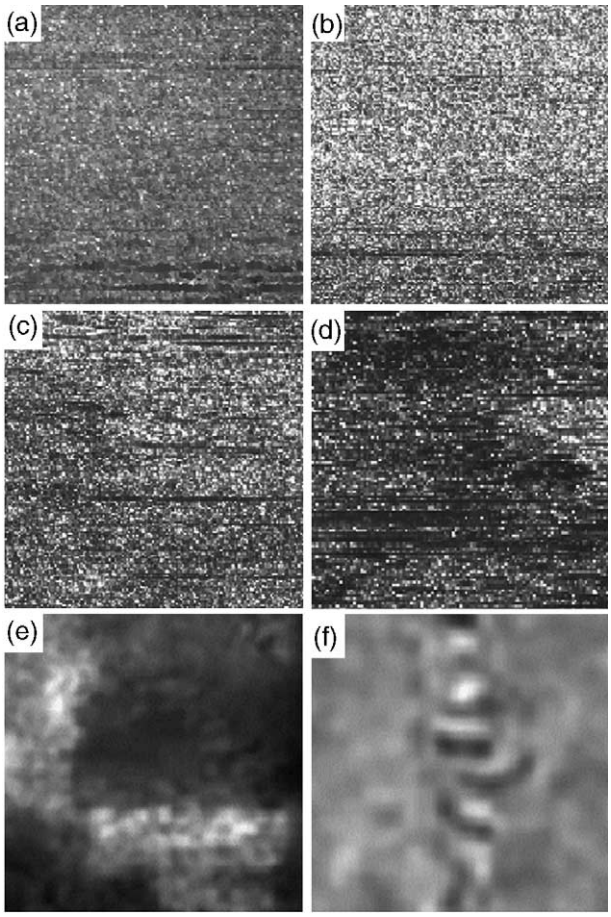

Fig. 5. AFM tapping phase image for EVOH-*g*-SPEG with different length of side chain: (a) $n=2$ dry membrane; (b) $n=2$ wet membrane; (c) $n=3$ wet membrane; (d) $n=4$ wet membrane; (e) $n=5$ wet membrane; (f) $n=6$ wet membrane. Scan boxes are 500×500 nm.

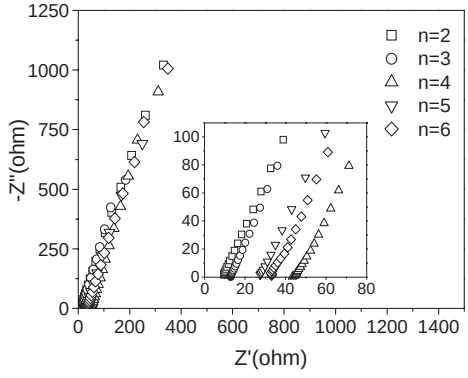

Fig. 6. Nyquist impedance plots of EVOH-*g*-SPEG with different length of side chain.

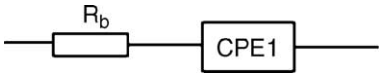

Fig. 7. An equivalent circuit to interpret the Nyquist impedance plots in Fig. 6.

stretching of S=O bond. The antisymmetric vibration of $-SO_3^-$ absorbance is at 1264 cm^{-1} and the symmetric vibration of this bond is at 1150~1185 cm^{-1}. The results proves that the PEG segment have been grafted onto the EVOH main chain, and the sulfonate groups were introduced to the end of the PEG side chain.

3.3. Water sorption of EVOH-g-SPEG membrane

The membrane hydration is closely related with the conductivity and the mechanical stability. The water uptakes of the membranes with different side chains length are given in Fig. 2. From Fig. 2, it is observed that the water sorption of the membranes depend on the length of PEG side chain. The longer the side chain of the electrolyte is, the greater the water uptake is. The water sorption of the membranes also increase with the immersion time (Fig. 3). It takes more than 12 h to reach the saturated water sorption for $n=2$, while for $n=3$ is 10 h; $n=4$, 8 h; $n=5$, 4 h; $n=6$, 0.15 h. The reason for the changes may come from the introduction of the side chain: first, the alkylene oxide and the sulfonic group in the side chain are hydrophilic group which could make the polymer electrolyte absorb more water; second, the side chain could destroy the crystallization of the main chain and increase the free volume between the molecular. The longer the side chain is, the bigger the free volume is, so the water sorption becomes greater.

3.4. XRD analysis of EVOH-g-SPEG membrane

The XRD results of dry and wet polymer membrane with grafted PEG ($n=2$) are shown in Fig. 4. Both films were quenched before measured. On curve a, there is a sharp diffraction peak at $2\theta=19.4°$ and two board diffraction peaks at $2\theta=5–13°$ and $2\theta=36–45°$, respectively. All of these diffraction peaks attribute to the crystallization of the main chain. On curve b, the strong sharp diffraction peak shifts from 2 $\theta=19.4°$ to 2 $\theta=20.2°$ and becomes a weak wide diffraction peak. That indicates the water in wet membrane could change the crystalline state and decrease crystallinity of SPE, whereas the low crystallinity is beneficial for the ion conductivity.

3.5. AFM analysis of EVOH-g-SPEG membrane

In order to determine the water state in the SPE membrane, AFM analysis is used. Fig. 5 shows the morphology of EVOH-*g*-SPEG with different length of the side chain. In these AFM phase images, the dark structures had larger phase lag and were assigned to a noncrystalline domain, which represents the hydrophilic PEG side chain and the sulfonic acid groups containing a larger fraction of water; brighter phase structure were assigned to a crystalline domain, which represents the hydrophobic EVOH main chain. For the dry membranes, i.e. $n=2$ dry membrane (Fig. 5a), featureless phase morphology was observed. On the other hand, for wet membranes, dark, cluster-like structures with an average diameter of 10~35 nm were clearly visible in the phase image. The dark structures were assigned to a softer region, which represents the hydrophilic PEG and sulfonic acid groups containing small amounts of water. The domain size varies with the length of the side chain. For $n=2$, an isolated ionic cluster region formed with an average diameter of 10~15 nm in the wet hydration film, for $n=3$ and $n=4$, the phase contrast of the hydrophilic ionic domains increased and became more easily distinguished from the non-ionic matrix, but the domains were still segregated with approximately 25 and 35 nm average diameters, respectively. The cluster-like structures which is known as cluster agglomerates is similar to Nafion 117 ionomer, although the cluster agglomerates size of the Nafion was about 30 nm. However, for $n=5$ and $n=6$ samples, the phase image undergoes a significant change, wherein the hydrophilic ionic domains become continuous to form large channels of an ionic rich phase.

3.6. Electrochemical impedance spectroscopy analysis

In order to understand the conductive behavior of the polymer electrolyte, electrochemical impedance spectroscopy (EIS) analysis of different membranes was performed. The impedance plots (Nyquist form) for the single ion polymer electrolyte with different length of side chain are shown in Fig. 6. In the Nyquist impedance plot, the imaginary part (Z'') of impedance is plotted as a function of its real component (Z') in the frequency range from 100 kHz to 10 Hz. In the typical Nyquist impedance plot, the straight line at low-frequency and the semicircle at high-frequency correspond to the electrolyte/electro interface impedance and bulk electrochemistry impedance, respectively. In Fig. 6, the Nyquist impedance of EVOH-*g*-SPEG polymer electrolyte shows a straight line during all frequency range. As reported

Table 3
Parameters for the circuit elements evaluated by fitting the impedance data of Fig. 6 to the equivalent circuit shown in Fig. 7

Sample	Fitted parameters			Calculated conductivity	
	CPE1-P (n)	CPE1-T (10^{-5} F)	R_b (Ω)	d/S (10^{-2} cm^{-1})	σ (10^{-4} S cm^{-1})
EVOH-*g*-SPEG ($n=2$)	0.823	0.907	10.17	1.681	16.5
EVOH-*g*-SPEG ($n=3$)	0.831	5.519	13.88	1.238	8.92
EVOH-*g*-SPEG ($n=4$)	0.822	3.542	44.93	0.947	2.11
EVOH-*g*-SPEG ($n=5$)	0.819	5.075	27.1	1.185	4.37
EVOH-*g*-SPEG ($n=6$)	0.822	3.167	33.1	1.150	3.04

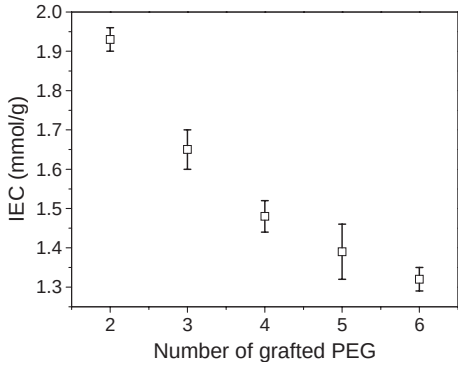

Fig. 8. IEC value of different lengths of side chains.

in the literature [25], the appearance of high-frequency semicircle should be higher than 100 kHz. However, the frequency requirement is beyond the instrument in our study.

The Nyquist plots agree well with the experiment data when equivalent circuit shown as Fig. 7 is adopted. The equivalent circuit consists of the bulk electrolyte resistance in series with the constant phase element CPE1. The constant phase element was the rough geometry interface [26,27]. CPE1 is given as necessarily introduced to account for the non-ideality of the interface between the electrode and electrolyte in the practical impedance spectrum, especially for an empirical formula:

$$Z_{CPE} = A(j\omega)^{-n} \tag{1}$$

$$\alpha = (1-n)\frac{\pi}{2} \tag{2}$$

where $A = C^{-1}$ only when $n = 1$, and n is related to α (the deviation from the vertical of the line in Nyquist plot), $n = 1$ indicates a perfect capacitance, and lower n values directly reflect the roughness of the electrode used.

Hence, with the help of the ZSimpWin software, the equivalent circuit was used to fit the experiment data. The bulk electrolyte resistance R_b and CPE1 can be estimated from this fitting procedure. The ionic conductivity δ of the SPE is calculated

$$\sigma = \frac{d}{R_b \times S} \tag{3}$$

where d is the thickness of the SPE film and S is the area of the SS electrode. The fitting parameters using the equivalent circuit (Fig. 7) are shown in Table 3.

The bulk resistance of $n = 2 \sim 6$ is 10.17, 13.88, 44.93, 27.1 and 33.1, respectively. And the ionic conductivity can be obtained by using Eq. (3). The conductivity generally decreases with the side chain length. But following the minimum conductivity at $n = 4$, the conductivity increases for longer side chain length, i.e. $n = 5$, $n = 6$. This feature is the reflection of two opposite effect, namely the decrease in ion densities and increase in water sorption of the SPE membrane. With the increasing of the side chain length, the IEC value of SPE will decrease (Fig. 8), and the ion densities in the polymer electrolytes decrease correspondingly with the IEC value which leads to decreasing of the ionic conductivity. At the same time, the water sorption increased with the side chain length. As shown in AFM phase images (Fig. 5e, f) when $n \geq 5$ the hydrophilic ionic domains become continuous to form large channels and cluster agglomeration, which is better for ion conductivity. In an addition, the XRD results indicate that water in wet membrane could decrease crystallinity of SPE which is also beneficial for the ion conductivity. So the effect from the decreasing of the ion densities carriers will dominate with $n \leq 4$, whereas the effect from the increasing of water sorption will takes precedence with $n \geq 5$. All of above cause the highest ionic conductivity appear when n is 2, and the lowest ionic conductivity is appear when n is 4.

4. Conclusion

EVOH-*g*-SPEG comb-like single ion electrolyte containing controllable PEG side chain ended with sulfonic acid was successfully prepared with the length of the side chain ranging from 2 to 6. The saturation water sorption in EVOH-*g*-SPEG membrane increased with the side chain length and the immersion time. The XRD results suggest that water absorbed by the membrane could decrease the crystallinity of the membrane. And AFM phase images showed that the hydrophilic ionic domains increased with diameter from 10 to 35 nm and connected together to form a continuous phase with $n \geq 5$. Because of the complex influence from the side chain length, the IEC value and the water sorption, the highest ionic conductivity of the EVOH-*g*-SPEG membrane would be 1.65×10^{-3} S cm^{-1} with $n = 2$, whereas the lowest ionic conductivity would be 2.11×10^{-4} S cm^{-1} with $n = 4$ according to the result of AC impedance.

Acknowledgments

This work was carried out under grant No. E0227 from Heilongjiang Nature Science Foundation and No. 10551078 from the Heilongjiang Education Bureau, People's Republic of China.

References

[1] D.E. Fenton, J.M. Parker, P.V. Wright, Polymer 14 (1973) 589.
[2] M. Armand, Solid State Ionics 10 (1983) 745.
[3] J.L. Acosta, E. Morales, J. Appl. Polym. Sci. 60 (1996) 1185.
[4] M. Mastragostino, C. Arbizzani, L. Meneghelo, R. Paraventi, Adv. Mater. 4 (1996) 331.
[5] A. Rudge, J. Davey, I. Raistrick, S. Gottesfeld, J.P. Ferraris, J. Power Sources 89 (1994) 47.
[6] M.A. De Paoli, A. Zanelli, M. Mastragostino, A.M. Rocco, J. Electroanal. Chem. 435 (1997) 217.
[7] Masayoshi Watanabe, Yusuke Suzuki, Astuishi Nishimoto, Electrochim. Acta 45 (2000) 1187.
[8] J.J. Sumner, S.E. Creager, J.J. Ma, D.D. DesMaryeau, J. Electrochem. Soc. 145 (1998) 107.
[9] D.J. Bannister, G.R. Davies, I.M. Ward, J.E. McIntyre, Polymer 25 (1984) 1291.
[10] M. Watanabe, Y. Suzuki, A. Nishimoto, Electrochim. Acta 45 (2000) 1187.
[11] K. Ito, H. Ohno, Solid State Ionics 79 (1995) 300.
[12] D.P. Siska, D.F. Shriver, Chem. Mater. 13 (2001) 4698.
[13] W. Xu, C.A. Angell, Solid State Ionics 147 (2002) 295.

[14] X.G. Sun, C.A. Angell, Solid State Ionics 175 (2004) 743.
[15] T. Fujinami, A. Tokimune, M.A. Mehta, D.F. Shriver, G.C. Rawsky, Chem. Mater. 9 (1997) 2236.
[16] E. Tsuchida, N. Kobayashi, H. Ohno, Macromolecules 21 (1988) 96.
[17] N.S. Choi, Y.M. Lee, B.H. Lee, J.A. Lee, J.K. Park, Solid State Ionics 167 (2004) 293.
[18] M.M. Doeff, J.S. Reed, Solid State Ionics 115 (1998) 109.
[19] G. Sandi, K.A. Carrado, H. Joachin, W. Lu, J. Prakash, J. Power Sources 119 (2003) 492.
[20] R.G. Singhal, M.D. Capracotta, J.D. Martin, S.A. Khan, P.S. Fedkiw, J. Power Sources 128 (2004) 247.
[21] N. Munichandraiah, L.G. Scanlon, R.A. Marsh, B. Kumar, A.K. Sircar, Electrochim. Acta 48 (2003) 2071.
[22] H. Derand, B. Wesslen, B.E. Mellander, Electrochim. Acta 43 (1998) 1525.
[23] J. Cowie, K. Sadaghianizadeh, Solid State Ionics 42 (1990) 243.
[24] U. Lauter, W.H. Meyer, G. Wegner, Macromolecules 30 (1997) 2092.
[25] H.J. Walls, M.W. Riley, P.S. Fedkiw, R.J. Spontak, G.L. Baker, S.A. Khan, J. Appl. Electrochem. 25 (1995) 857.
[26] R.O. Ansel, T. Dickinson, A.F. Povy, P.M.A. Sherwood, J. Electrochem. Soc. 124 (1977) 1360.
[27] M.J. Rodiguez Presa, R.I. Tuueri, M.I. Florit, D. Posaldas, J. Electroanal. Chem. 82 (2001) 502.